

Three modulation patterns in four related $[M(\text{H}_2\text{O})_2(15\text{-crown-5})](\text{NO}_3)_2$ structures

Xiang Hao, Sean Parkin and
Carolyn Pratt Brock*

Department of Chemistry, University of
Kentucky, Lexington, KY 40506-0055, USA

Correspondence e-mail: cpbrock@uky.edu

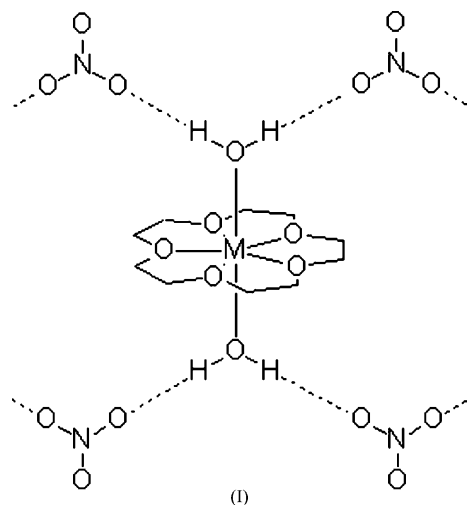
Received 1 July 2005

Accepted 19 August 2005

The structures of $[M(\text{H}_2\text{O})_2(15\text{-crown-5})](\text{NO}_3)_2$, $M = \text{Cu}$, Zn , Mg and Co , and 15-crown-5 = 1,4,7,10,13-pentaoxacyclopentadecane, have been redetermined at 294 and 90 K. The four structures, and a second form of the Cu structure, have been reported in the literature, but are all incorrect in some significant way. The structures, which all have at least two independent formula units (*i.e.* $Z' \geq 2$), are related; each water ligand is hydrogen-bonded to two nitrate anions, while each nitrate anion is hydrogen bonded to the water ligands of two cations. In the tetragonal Co structure the hydrogen-bond pattern is three-dimensional; in the monoclinic Cu, Zn and Mg structures the hydrogen-bond patterns are two-dimensional. In the isostructural Zn and Mg structures $Z' = 3$, while in the Cu structure $Z' = 5$. The Cu, Zn and Mg structures are modulated variants of a basic structure, which was reported for Cu but which probably does not exist. The conformations of the 11 independent cations are remarkably similar; they all have approximate twofold symmetry and so exist as conformational enantiomers. The most important modulation is imperfect enantiomeric alternation of the cations along the longest cell axis; the independent cations are related by very good pseudotranslation and pseudoinversion operations. The diffraction patterns for all four structures have classes of weak, even very weak, reflections.

1. Introduction

This project was begun because we wondered whether the room-temperature structures with refcodes GAVPEY (Pc , $Z' = 10$; Dejehet *et al.*, 1987b) and GAVPEY01 ($P2_1/c$, $Z' = \frac{1}{2}$; Rogers & Song, 1995) of $[\text{Cu}(\text{H}_2\text{O})_2(15\text{-crown-5})](\text{NO}_3)_2$ found in the Cambridge Structural Database (Allen, 2002; hereafter, the CSD) were different polymorphs. The packing seemed to be the same in the two structures, so it was not clear whether the two were closely related polymorphs or whether a mistake had been made in one of the structure determinations. The reduced cells for the two reported structures are related (see Schönleber & Chapuis, 2004): the length of the unique axis and the monoclinic angle are almost the same in the two cells, and the lengths of the two other axes are related by factors of 2.00 and 4.89. On the other hand Rogers & Song (1995) wrote 'A crystal structure of the latter complex has been published, however, we were unable to reproduce the unit cell obtained in that study'. We decided to investigate the problem further.



In the course of studying the $M = \text{Cu}$ compound we found three related structures in the CSD. The corresponding Zn compound (FETPEZ; Dejehet *et al.*, 1987*a*) was reported to crystallize at room temperature in a structure similar to the Cu compound, but with $Z' = 6$ rather than 10. The unit cell of the $M = \text{Mg}$ compound (JAWQIH; Junk & Steed, 1999) seemed to be similar to those of the Cu and Zn compounds, but the space group was given as $P2_1/c$ rather than as Pc , and Z' was reported to be $3 = 2 + 2(\frac{1}{2})$ with two of the four independent cations disordered over inversion centers. The $M = \text{Co}$ compound (CLCOPC10; Holt *et al.*, 1981) was reported to be disordered in the $P4_12_12$ group with $Z' = \frac{1}{2}$, but no coordinates are archived in the Cambridge Structural Database (CSD).

All of these structures, most of which were determined some years ago, warranted another look. All were found to be incorrect in some way. Inversion centers should be added to both the Zn structure and the modulated Cu structure so that the Z' values are reduced to 3 and 5 from 6 and 10. We could find no evidence for the Cu phase with the smaller (and disordered) unit cell. An origin shift resolves the disorder in the Mg compound, which is then found to be isostructural with the Zn compound. The observation of weak reflections for the Co compound shows that the cell is twice as large as reported, that the symmetry is lower than described and that the structure is an ordered merohedral twin.

Investigation of these compounds led to the discovery of a large system of related structures that all have $Z' > 1$. [Additional, higher-temperature phases of the Mg, Zn and Cu compounds will be discussed in a later paper, as will the phases of the analogous Mn, Fe and Ni compounds (Hao *et al.*, 2005*a,b*)]. This paper begins a discussion of this system of related compounds and then examines the reasons for the problems with the original structure determinations.

2. Experimental

Crystals were grown by evaporation from aqueous solutions (except as noted below), equimolar in 15-crown-5 ether

(1,4,7,10,13-pentaoxacyclopentadecane) and $M(\text{NO}_3)_2 \cdot n\text{H}_2\text{O}$, with $n = 3$ for $M = \text{Cu}$ and $n = 6$ for $M = \text{Zn}, \text{Mg}$ and Co . Crystals of the Cu, Zn and Mg compounds were colorless; crystals of the Co compound were purple. We were initially surprised that the Cu-containing crystals were not blue, but found that the electronic spectroscopy of the compound had been studied and explained (Li, 1996).

Data for each of the four crystals were collected at room temperature and near 90 K with a Nonius KappaCCD diffractometer equipped with a CRYOCOOL-LN2 low-temperature system (CRYO Industries of America, Manchester, NH). Crystals were first cooled from room temperature in the standard way (*i.e.* within several seconds), but later experiments showed that slow cooling (< 0.5 K per minute) did not identify any new phase transition for the Cu, Zn or Mg compounds (although it did for the analogous Mn and Fe compounds). The possibility that some of the modulations found in these crystals might be incommensurate was considered but ruled out. All of the diffraction maxima had integral indices for unit cells that were integer multiples of a basic pseudocell. There were no particular problems indexing any of the diffraction patterns, and reciprocal-lattice slices reconstructed from the raw data frames had no unexpected or unexplained features. In general, the least-squares refinements of the structures were carried out first at the lower temperature because the $I/\sigma(I)$ ratios were better and the deviations from pseudosymmetry larger. Results of the room-temperature refinements, which were in some cases problematic because of weak data and high correlations, are included to allow comparisons with published structures. Separate Wilson plots were made for the strong and weak reflections for each structure at each temperature (see Xia *et al.*, 2001, 2002); some of these plots are given (see below) and the others are available with the supplementary material.¹ Some details of the data collection and structure refinement are given in Table 1.

The methylene H atoms were placed at calculated positions ($r_{\text{C-H}} = 0.99$ Å near 90 K and 0.97 Å near room temperature) and allowed to ride on the attached C atom (AFIX 23; $U_{\text{H}} = 1.2U_{\text{iso}}$ of the C atom). The H atoms of the water ligands for the low-temperature structures were located in difference Fourier maps and refined with restraints. A single free parameter was refined for all four O—H distances and for the two H...H distances divided by 1.58 Å (1.58 is twice the sine of half of the target H—O—H angle of 104.5°). The final values of these variables are shown in Table 1. All refinements of room-temperature data started from the converged low-temperature refinements and used (except as noted below) the same restraints.

In the three structures with $Z' > 2$ the option in *SHELXL* (Sheldrick, 1997*b*) for using residue numbers proved very useful. All atoms have labels of the form Xi_j , where X is the atom type, i is the atom number and j is the residue number. The atom-numbering scheme for the C and O atoms is the

¹ Supplementary data for this paper are available from the IUCr electronic archives (Reference: BM5026). Services for accessing these data are described at the back of the journal.

Table 1
Experimental data.

Comment: The space group symbols will be rendered correctly if the CIF contains no brackets in the symbol, for example 'P 21/c' rather than 'P2(1)/c'

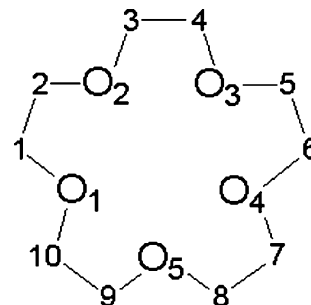
	Cu RT	Cu LT	Zn RT	Zn LT
Crystal data				
Chemical formula	C ₁₀ H ₂₄ CuN ₂ O ₁₃	C ₁₀ H ₂₄ CuN ₂ O ₁₃	C ₁₀ H ₂₄ N ₂ O ₁₃ Zn	C ₁₀ H ₂₄ N ₂ O ₁₃ Zn
<i>M_r</i>	443.85	443.85	445.68	445.68
Cell setting, space group	Monoclinic, <i>P</i> ₂ ₁ / <i>n</i>	Monoclinic, <i>P</i> ₂ ₁ / <i>n</i>	Monoclinic, <i>P</i> ₂ ₁ / <i>c</i>	Monoclinic, <i>P</i> ₂ ₁ / <i>c</i>
<i>a</i> , <i>b</i> , <i>c</i> (Å)	14.772 (3), 13.987 (3), 43.344 (9)	14.659 (3), 14.029 (3), 42.475 (9)	14.721 (3), 14.077 (3), 26.111 (5)	14.633 (3), 14.034 (3), 25.561 (5)
β (°)	97.33 (3)	96.85 (3)	96.83 (3)	96.48 (3)
<i>V</i> (Å ³)	8883 (3)	8673 (3)	5372.4 (18)	5215.6 (18)
<i>Z</i>	20	20	12	12
<i>D_x</i> (Mg m ⁻³)	1.659	1.700	1.653	1.703
Radiation type	Mo <i>K</i> α	Mo <i>K</i> α	Mo <i>K</i> α	Mo <i>K</i> α
No. of reflections for cell parameters	18 790	27 941	12 798	12 391
θ range (°)	1.0–25.0	1.0–25.4	1.0–27.5	1.0–27.5
μ (mm ⁻¹)	1.30	1.33	1.44	1.48
Temperature (K)	294 (2)	88.0 (2)	294 (2)	90.0 (2)
Crystal form, color	Block, colorless	Block, colorless	Block, colorless	Block, colorless
Crystal size (mm)	0.30 × 0.30 × 0.25	0.50 × 0.30 × 0.10	0.30 × 0.20 × 0.10	0.20 × 0.10 × 0.10
Data collection				
Diffractometer	Nonius KappaCCD diffractometer	Nonius KappaCCD diffractometer	Nonius KappaCCD diffractometer	Nonius KappaCCD diffractometer
Data collection method	ω scans at fixed $\chi = 55^\circ$	ω scans at fixed $\chi = 55^\circ$	ω scans at fixed $\chi = 55^\circ$	ω scans at fixed $\chi = 55^\circ$
Absorption correction	Multi-scan (based on symmetry-related measurements)	Multi-scan (based on symmetry-related measurements)	Multi-scan (based on symmetry-related measurements)	Multi-scan (based on symmetry-related measurements)
<i>T_{min}</i>	0.697	0.556	0.672	0.756
<i>T_{max}</i>	0.737	0.878	0.869	0.866
No. of measured, independent and observed reflections	42 944, 15 225, 3609	31 464, 15 865, 6966	18 511, 9469, 4071	17 973, 9195, 5267
Criterion for observed reflections	<i>I</i> > 2σ(<i>I</i>)	<i>I</i> > 2σ(<i>I</i>)	<i>I</i> > 2σ(<i>I</i>)	<i>I</i> > 2σ(<i>I</i>)
<i>R_{int}</i>	0.082	0.041	0.047	0.035
θ_{\max} (°)	25.1	25.4	25.0	25.0
Range of <i>h</i> , <i>k</i> , <i>l</i>	−17 ⇒ <i>h</i> ⇒ 17 −16 ⇒ <i>k</i> ⇒ 16 −51 ⇒ <i>l</i> ⇒ 51	−17 ⇒ <i>h</i> ⇒ 17 0 ⇒ <i>k</i> ⇒ 16 −51 ⇒ <i>l</i> ⇒ 51	−17 ⇒ <i>h</i> ⇒ 17 −16 ⇒ <i>k</i> ⇒ 16 −31 ⇒ <i>l</i> ⇒ 30	−17 ⇒ <i>h</i> ⇒ 17 −16 ⇒ <i>k</i> ⇒ 16 −30 ⇒ <i>l</i> ⇒ 30
Refinement				
Refinement on	<i>F</i> ²	<i>F</i> ²	<i>F</i> ²	<i>F</i> ²
<i>R</i> [<i>F</i> ² > 2σ(<i>F</i> ²)], <i>wR</i> (<i>F</i> ²), <i>S</i>	0.055, 0.208, 0.86	0.043, 0.116, 0.99	0.040, 0.107, 0.91	0.033, 0.085, 0.93
No. of reflections	15 225	15 865	9469	9195
No. of parameters	547	1232	740	740
H-atom treatment	Constrained to parent site	Mixture of independent and constrained refinement	Mixture of independent and constrained refinement	Mixture of independent and constrained refinement
⟨O–H⟩ and ⟨H··H⟩ in water (Å)	Fixed at 0.77	0.766 (9)	0.779 (13)	0.781 (10)
Weighting scheme	$w = 1/[\sigma^2(F_o^2) + (0.0795P)^2]$, where $P = (F_o^2 + 2F_c^2)/3$	$w = 1/[\sigma^2(F_o^2) + (0.045P)^2]$, where $P = (F_o^2 + 2F_c^2)/3$	$w = 1/[\sigma^2(F_o^2) + (0.044P)^2]$, where $P = (F_o^2 + 2F_c^2)/3$	$w = 1/[\sigma^2(F_o^2) + (0.0357P)^2]$, where $P = (F_o^2 + 2F_c^2)/3$
(Δ/ σ) _{max}	0.003	0.002	0.002	0.001
Δρ _{max} , Δρ _{min} (e Å ⁻³)	0.60, −0.66	0.50, −0.47	0.33, −0.54	0.36, −0.56
Extinction method	None	None	None	None
<hr/>				
	Mg RT	Mg LT	Co RT	Co LT
Crystal data				
Chemical formula	C ₁₀ H ₂₄ MgN ₂ O ₁₃	C ₁₀ H ₂₄ MgN ₂ O ₁₃	C ₁₀ H ₂₄ CoN ₂ O ₁₃	C ₁₀ H ₂₄ CoN ₂ O ₁₃
<i>M_r</i>	404.62	404.62	439.24	439.24
Cell setting, space group	Monoclinic, <i>P</i> ₂ ₁ / <i>c</i>	Monoclinic, <i>P</i> ₂ ₁ / <i>c</i>	Tetragonal, <i>P</i> ₄ ₁	Tetragonal, <i>P</i> ₄ ₁
<i>a</i> , <i>b</i> , <i>c</i> (Å)	14.601 (3), 14.182 (3), 26.241 (5)	14.497 (3), 14.181 (3), 25.700 (5)	11.4250 (16), 11.4250 (16), 27.248 (5)	11.3055 (16), 11.3055 (16), 27.041 (5)
β (°)	96.77 (3)	96.46 (3)	90.00	90.00
<i>V</i> (Å ³)	5396.0 (19)	5249.9 (18)	3556.7 (10)	3456.2 (10)
<i>Z</i>	12	12	8	8
<i>D_x</i> (Mg m ⁻³)	1.494	1.536	1.641	1.688
Radiation type	Mo <i>K</i> α	Mo <i>K</i> α	Mo <i>K</i> α	Mo <i>K</i> α

Table 1 (continued)

	Mg RT	Mg LT	Co RT	Co LT
No. of reflections for cell parameters	12 854	23 626	8528	15 108
θ range ($^\circ$)	1.0–27.5	1.0–27.5	1.0–27.5	1.0–27.5
μ (mm^{-1})	0.17	0.17	1.03	1.06
Temperature (K)	294 (2)	90.0 (2)	294 (2)	90.0 (2)
Crystal form, color	Block, colorless	Block, colorless	Block, purple	Plate, purple
Crystal size (mm)	0.30 \times 0.20 \times 0.10	0.30 \times 0.20 \times 0.10	0.40 \times 0.30 \times 0.30	0.30 \times 0.20 \times 0.05
Data collection				
Diffractometer	Nonius KappaCCD diffractometer	Nonius KappaCCD diffractometer	Nonius KappaCCD diffractometer	Nonius KappaCCD diffractometer
Data collection method	ω scans at fixed $\chi = 55^\circ$	ω scans at fixed $\chi = 55^\circ$	ω scans at fixed $\chi = 55^\circ$	ω scans at fixed $\chi = 55^\circ$
Absorption correction	Multi-scan (based on symmetry-related measurements)	Multi-scan (based on symmetry-related measurements)	Multi-scan (based on symmetry-related measurements)	Multi-scan (based on symmetry-related measurements)
T_{\min}	0.951	0.950	0.682	0.741
T_{\max}	0.983	0.983	0.747	0.949
No. of measured, independent and observed reflections	18 536, 9497, 3115	46 462, 12 054, 5815	17 230, 6261, 3814	23 271, 6076, 4216
Criterion for observed reflections	$I > 2\sigma(I)$	$I > 2\sigma(I)$	$I > 2\sigma(I)$	$I > 2\sigma(I)$
R_{int}	0.081	0.103	0.072	0.135
θ_{max} ($^\circ$)	25.0	27.5	25.0	25.0
Range of h, k, l	$-17 \Rightarrow h \Rightarrow 17$ $-16 \Rightarrow k \Rightarrow 16$ $-31 \Rightarrow l \Rightarrow 31$	$-18 \Rightarrow h \Rightarrow 18$ $-18 \Rightarrow k \Rightarrow 18$ $-33 \Rightarrow l \Rightarrow 33$	$-13 \Rightarrow h \Rightarrow 13$ $-11 \Rightarrow k \Rightarrow 13$ $-31 \Rightarrow l \Rightarrow 32$	$-13 \Rightarrow h \Rightarrow 13$ $-13 \Rightarrow k \Rightarrow 13$ $-32 \Rightarrow l \Rightarrow 32$
Refinement				
Refinement on	F^2	F^2	F^2	F^2
$R[F^2 > 2\sigma(F^2)], wR(F^2), S$	0.048, 0.137, 0.87	0.045, 0.106, 0.94	0.046, 0.096, 0.94	0.048, 0.075, 0.98
No. of reflections	9497	12 054	6261	6076
No. of parameters	740	740	369	495
H-atom treatment	Mixture of independent and constrained refinement	Mixture of independent and constrained refinement	Constrained to parent site	Mixture of independent and constrained refinement
$\langle \text{O} \cdots \text{H} \rangle$ and $\langle \text{H} \cdots \text{H} \rangle$ in water (\AA)	0.761 (12)	0.832 (8)	Fixed at 0.79	0.786 (16)
Weighting scheme	$w = 1/[\sigma^2(F_o^2) + (0.0513P)^2]$, where $P = (F_o^2 + 2F_c^2)/3$	$w = 1/[\sigma^2(F_o^2) + (0.0414P)^2]$, where $P = (F_o^2 + 2F_c^2)/3$	$w = 1/[\sigma^2(F_o^2) + (0.0348P)^2]$, where $P = (F_o^2 + 2F_c^2)/3$	$w = 1/[\sigma^2(F_o^2) + (0.0217P)^2]$, where $P = (F_o^2 + 2F_c^2)/3$
$(\Delta/\sigma)_{\text{max}}$	<0.0001	<0.0001	0.002	0.005
$\Delta\rho_{\text{max}}, \Delta\rho_{\text{min}}$ (e \AA^{-3})	0.25, -0.27	0.24, -0.28	0.41, -0.25	0.31, -0.32
Extinction method	None	None	SHELXL	None
Extinction coefficient	–	–	0.00177 (16)	–
Absolute structure	–	–	Flack (1983)	Flack (1983)
Flack parameter	–	–	-0.02 (2)	-0.004 (17)

Computer programs used: COLLECT (Nonius, 1999), SCALEPACK, DENZO-SMN (Otwinowski & Minor, 1997), SHELXS97 (Sheldrick, 1997a), SHELXL97 (Sheldrick, 1997b), XP in Siemens SHELXTL (Sheldrick, 1994) and local procedures. The s.u.s quoted here for cell dimensions have been artificially increased (see e.g. Herbst, 2000) by at least a factor of three over the values given by the cell-determination software. We note that at present there is no proper consensus on such treatment; indeed, opinions differ even among the authors of this paper.

same for all cations and for all anions. The C and O atoms of the crown ligand are numbered as shown in the scheme below, while O6 and O7 are the O atoms of the water ligands. Atoms O8, O9 and O10 belong to the nitrate anions. It was necessary to give sequential numbers to one atom per ion (the M or N atom) so that each ion could be identified when display programs that do not recognize residue numbers (e.g. XP in SHELXTL; Sheldrick, 1994) were used. The atom numbers of the M ions (atomic scattering factors used) are the same as their residue numbers; the atom numbers of the N atoms go from 1 to 2Z' for residues Z' + 1 to 3Z', where Z' is 5 for the Cu compounds and 3 for the Zn and Mg compounds.



2.1. $M = \text{Cu}$

The large ($Z = 20$) monoclinic cell reported by Dejehet *et al.* (1987*b*) was found for all the crystals examined (see below). As that Pc cell had an obvious pseudotranslation along the cell diagonal $\mathbf{a} + \mathbf{c}$, as well as a weaker pseudotranslation along \mathbf{a} , the Pc cell was transformed to a Pn cell so that the pseudotranslation would be $\mathbf{c}/5$. This transformation leaves a and b unchanged and shortens c by only 1.5%, but changes β from 102.2 to 97.3°. Refinements in both Pc and Pn , however, were unsatisfactory, with many correlation coefficients close to ± 1 . The structure was therefore solved again with *SHELXS* (Sheldrick, 1997*a*) in the space group $P2_1/n$. The origin and asymmetric unit were chosen, and the atoms numbered, in a way that reflects the pseudosymmetry (see Fig. 1).

The data measured near 90 K could be refined without any restraints (other than those mentioned above for the water H atoms); no correlation coefficient had an absolute value larger than 0.64. Refinement of the room-temperature data, however, required constraints because the intensities of many of the superstructure peaks are very weak (see below); overall, only 24% of the data have $I > 2\sigma(I)$ at 294 K, while 44% do near 90 K. For the crown and water ligands at 294 K, displacement ellipsoids of the five C atoms or the five O atoms of each set of atoms related by pseudo-translations and pseudo-inversions (*e.g.*, C1_ j , $j = 1-5$) were required to be the same. For the nitrate ions the ellipsoids for each of the four sets of ten atoms (one atom from each of ten anions in each set) related by pseudotranslation and pseudo-inversion were also

required to be the same. The H atoms of the water ligand were fixed in positions similar to those found in the low-temperature structure. Absolute values of correlation coefficients were as large as 0.78.

In attempts to try to find the $Z' = \frac{1}{2}$ polymorph crystals were grown from different solvents at room temperature (distilled water, methanol, mixtures of methanol and acetonitrile) and from water solutions at several different temperatures (294, 315 and 338 K). More than ten crystals were examined, all of which showed the diffraction peaks characteristic of the larger unit cell.

Since 'single' crystals containing two phases related by a modulation are known (*e.g.* Brock & Patrick, 2002), we investigated the possibility that the $Z' = 5$ and $Z' = \frac{1}{2}$ phases might both be present in at least one of the crystals examined. Comparisons of the Wilson plots, which were made separately for the hkl , $\ell = 5n$, $\ell = 5n \pm 1$ and $\ell = 5n \pm 2$ reflections, showed that the decrease of intensity with scattering angle was the same for all the Cu crystals examined (see Fig. 2). Diffracted intensities from a disordered phase would be expected to decrease more rapidly with scattering angle than intensities from an ordered phase. If a 'crystal' were a hybrid containing both disordered and ordered phases then the decrease in intensity with scattering angle should be greater than for a completely ordered crystal. We saw no significant differences between any of the Wilson plots. We concluded that none of the crystals examined contained a significant amount of the phase reported by Rogers & Song (1995).

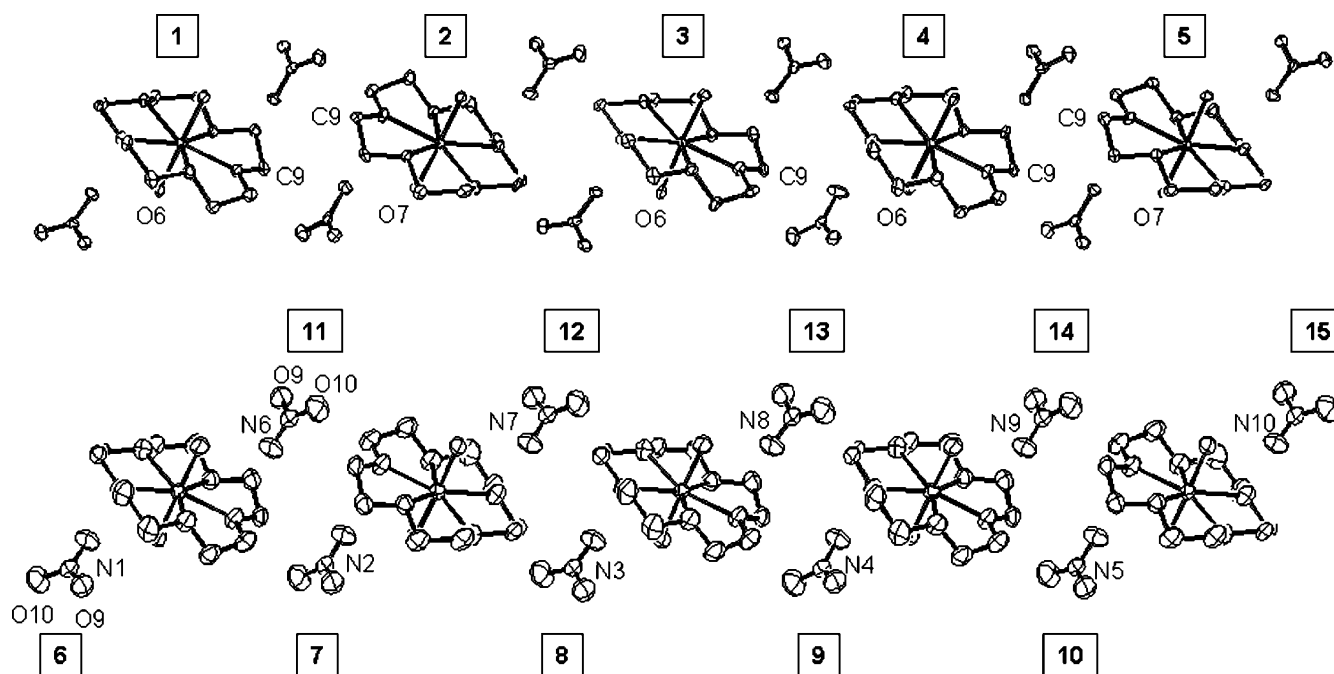


Figure 1

Perspective drawings of the asymmetric unit of the Cu compound, which is viewed along \mathbf{a} at 88 K (upper drawings) and 294 K (lower drawings). The \mathbf{c} axes are horizontal. Ellipsoids are drawn at the 50% level and H atoms have been omitted in this and all subsequent drawings. The atom-numbering schemes for the cation and anion are defined on the upper and lower drawings, respectively. The residue numbers are shown in boxes above or below the ions. The numbers for one C atom in each cation and two O atoms in each of two anions are shown; other atom numbers can be worked out from the translational pseudosymmetry ($\mathbf{c}/5$) and from the overall scheme described in the text.

Pseudocell refinements of the Cu structure were also made (see Xia *et al.*, 2001, 2002). All h indices were divided by two and all ℓ indices were divided by five; reflections with non-integral indices were then discarded. The coordinates of two enantiomeric cations and two anions (*e.g.* anions 6 and 11) could have been transformed to the pseudocell, but it was easier just to solve the structure again in the smaller unit cell (group $P2_1/c$; $Z' = \frac{1}{2}$; cation located on an inversion center and therefore disordered). The refinements in the pseudocell were very satisfactory. At 294 K the values of R_{int} , R and wR are 0.026, 0.033 and 0.108 for 1527 observations [of which 1221 have $I > 2\sigma(I)$]; at 88 K the corresponding values are 0.014, 0.023 and 0.060 for 1570 reflections, of which 1433 had $I > 2\sigma(I)$. The ellipsoids are somewhat larger than for the refinements using all the data, but the ellipsoids are neither

large enough nor eccentric enough to raise much suspicion. The low agreement factors and acceptable ellipsoids are possible because the $h = 2n$ and $\ell = 5n$ reflections are much more intense on average than the other reflections, and because the independent cations and anions in the true unit cell are related by very good pseudotranslations and pseudoinversions.

The possibility of a transition above 294 K of the $Z' = 5$ phase to a $P2_1/c$, $Z' = \frac{1}{2}$ phase was also investigated by crystallography and differential scanning calorimetry (DSC). When the $Z' = 5$ phase is heated it transforms at *ca* 312 K without the loss of crystallinity to an ordered triclinic phase with $Z' = 2$ that has also been found for $M = \text{Mn}$ (Hao *et al.*, 2005*a,b*). There is no indication of any other phase transformation near room temperature.

During the course of looking at the crystals of the Cu compound we had problems indexing some of the diffraction patterns, especially those produced by smaller crystals. The program *DENZO* (Otwinowski & Minor, 1997) sometimes found a *B*-centered cell (see later). This confusion could be avoided if the detector were moved back from the default distance of 40 mm to a much longer distance (80–90 mm). All sets of data were collected with Mo $K\alpha$ radiation at a detector distance of at least 80 mm.

2.2. $M = \text{Zn}$

The structure appears in the literature (Dejehet *et al.*, 1987*a*) in the space group *Pc*, but since the Cu structure turned out to be centrosymmetric, the Zn structure was solved again with *SHELXS* (Sheldrick, 1997*a*) in space group $P2_1/c$.

The $P2_1/c$ Zn structure ($Z' = 3$) is very like the $P2_1/n$ Cu structure ($Z' = 5$) except that the length of **c** is reduced by about 3/5. The origin and asymmetric unit were chosen, and the atoms were labeled, so that the locations of all ions, and the conformations of the three independent crown ligands, were consistent with those in the Cu structure (see Fig. 3).

The pseudotranslations along **a** and **c** did not interfere with the refinement, even though at room temperature and $(\sin \theta/\lambda)^2 = 0.10 \text{ \AA}^{-2}$ (*i.e.* $\theta = 13^\circ$ for Mo $K\alpha$ radiation) the $h0\ell$, $h = 2n$ reflections are about five times more intense than $h0\ell$, $h \neq 2n$ reflections and the $h0\ell$, $\ell = 3n$ are about ten times more intense than the $\ell \neq 3n$ reflections. At room temperature about 43% of the reflections have $I > 2\sigma(I)$; near 90 K this percentage rises to 53%. Absolute values of correlation coefficients were less than 0.67 and 0.57 at 90 and 294 K.

The final structure is consistent with that published by Dejehet *et al.* (1987*a*), except that inversion centers have been added.

2.3. $M = \text{Mg}$

The cell found in this study seems to be the same as reported by Junk & Steed (1999), but structure solution with *SHELXS* (Sheldrick, 1997*a*) suggested that the cell origin should be moved by about $\frac{1}{4}$ along **a**. The structure we found, which is ordered and isostructural with that of the Zn compound, was refined without difficulty to an R value of

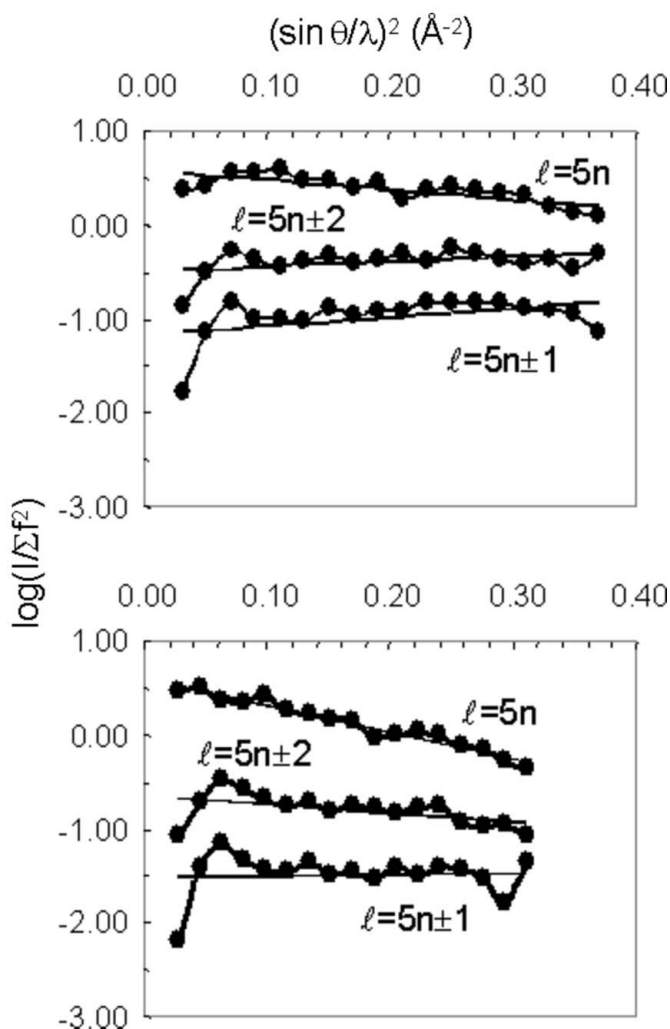


Figure 2
Wilson plots for the $\ell = 5n$, $\ell = 5n \pm 1$ and $\ell = 5n \pm 2$ reflections of the Cu compound as observed at 88 K (upper drawing) and 294 K (lower drawing). The absolute values of the vertical axis have relative significance only. The lines have been drawn as guides to the eye. The slopes of the lines for the $\ell = 5n \pm 1$ and $\ell = 5n \pm 2$ reflections at 88 K are positive because the increase in intensity with increasing resolution is more important than the decrease in intensity that results from thermal motion.

0.045 for data collected at 90 K (see Fig. 4); the R factor for the structure published previously is 0.117 for data collected at 100 K. Absolute values of correlation coefficients between least-squares parameters were less than 0.50 at 90 K and less than 0.61 at 294 K.

The Wilson plots suggest that the structure is less pseudosymmetric than the Zn structure, presumably because the Mg ion dominates the scattering less than the Zn ion does. At room temperature and 0.10 \AA^{-2} the $h0\ell$, $h = 2n$ reflections are about three times more intense than $h0\ell$, $h \neq 2n$ reflections; the ratio for the $h0\ell$, $\ell = 3n$ and $\ell \neq 3n$ reflections at the same scattering angle is *ca* 6:1. At room temperature about 33% of the reflections have $I > 2\sigma(I)$; near 90 K this percentage rises to 48%.

2.4. $M = \text{Co}$

Data collection revealed weak reflections corresponding to a unit cell related to the published cell (Holt *et al.*, 1981) by the matrix $(110/\bar{1}10/001)$. The hkl , $h + k = 2n$ reflections are about eight times more intense at 0.10 \AA^{-2} than are the hkl , $h + k \neq 2n$ reflections. At room temperature about 61% of the

reflections have $I > 2\sigma(I)$; near 90 K this percentage rises to 69%.

The symmetry of the larger unit cell is $P4_1$ (or $P4_3$) rather than $P4_12_12$ (or $P4_32_12$) as was reported earlier; if the space group were the latter, there would have to be twofold rotation axes parallel $[110]$, but those axes are clearly missing. As the cell is larger and the symmetry lower than reported earlier, Z' is 2 rather than $\frac{1}{2}$; the two independent cations are related by approximate C centering (see above), although if the centering were real the cation would be disordered. The cations and anions are also related by very good, although approximate, twofold screw axes parallel to \mathbf{b} at $x \text{ ca } \frac{1}{2}$ and $z \text{ ca } 0.11$ and 0.61 (the arbitrary z value corresponds to the coordinates reported in this study). There are less good approximate twofold screw axes parallel to \mathbf{a} at $y \text{ ca } 0.4$ and $z \text{ ca } 0.11 + \frac{1}{4}$ and $0.61 + \frac{1}{4}$. Local pseudo inversion centers are also present. Merohedral twinning [fractions 0.183 (2) for the crystal used at 90 K and 0.562 (3) for the crystal used at 294 K] was an additional complication.

At 90 K no restraints were applied (absolute values of all correlation coefficients < 0.70), although some of the ellipsoids were somewhat eccentric. The structure could not be refined at 294 K without fixing the H atoms of the water ligands in

positions corresponding to those found at 90 K, and relating the atomic displacement parameters for corresponding C and O atoms of the crown and water ligands that are related by the pseudo- 2_1 axis parallel to \mathbf{b} (17 atoms; 102 constraints). Free variables were used for 17 sets of six U^{ij} values because the pseudosymmetry operation that relates the two cations of the asymmetric unit requires that the U^{23} components of the corresponding atoms have opposite signs. Correlation coefficients involving the Co and nitrate ions were significant (absolute values as large as 0.86), perhaps because the twin fractions were so close to $\frac{1}{2}$. The final atomic ellipsoids are reasonable (see Fig. 5), although there are indications in both cations (large ellipsoids; short $C3n - C4n$ distance) of an up/down disorder in one C_2H_4 unit.

The atom-numbering scheme for this structure was chosen differently than for the other structures so that the restraints could be applied in a logical way. The two cations have very similar conformations (see below), but the orientations of the cations that give the best superposition fit are not

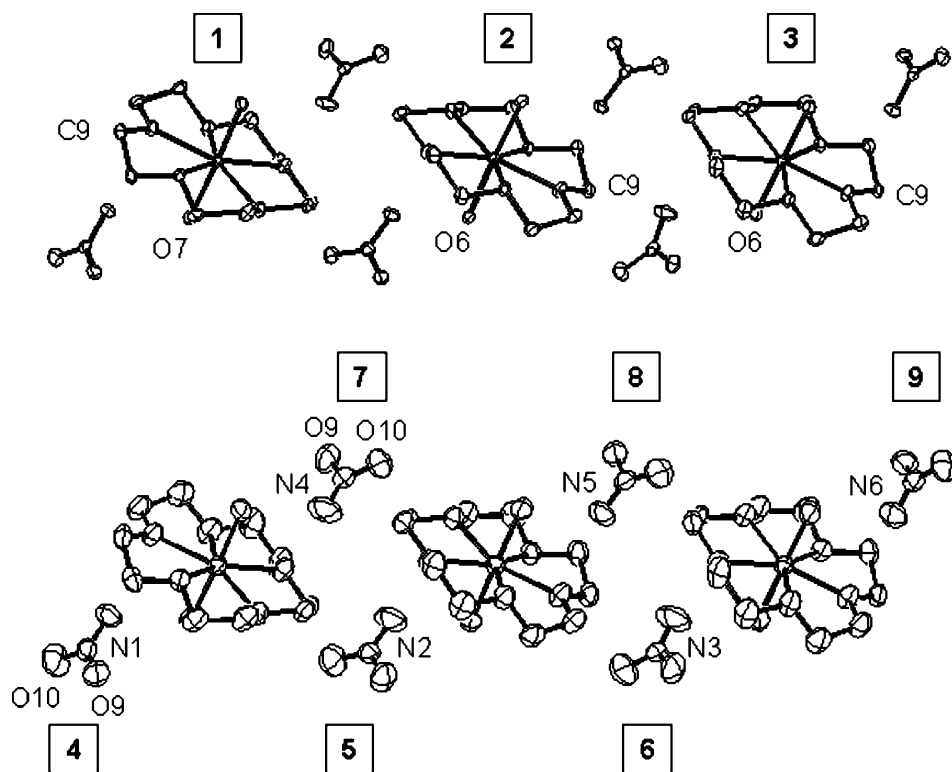
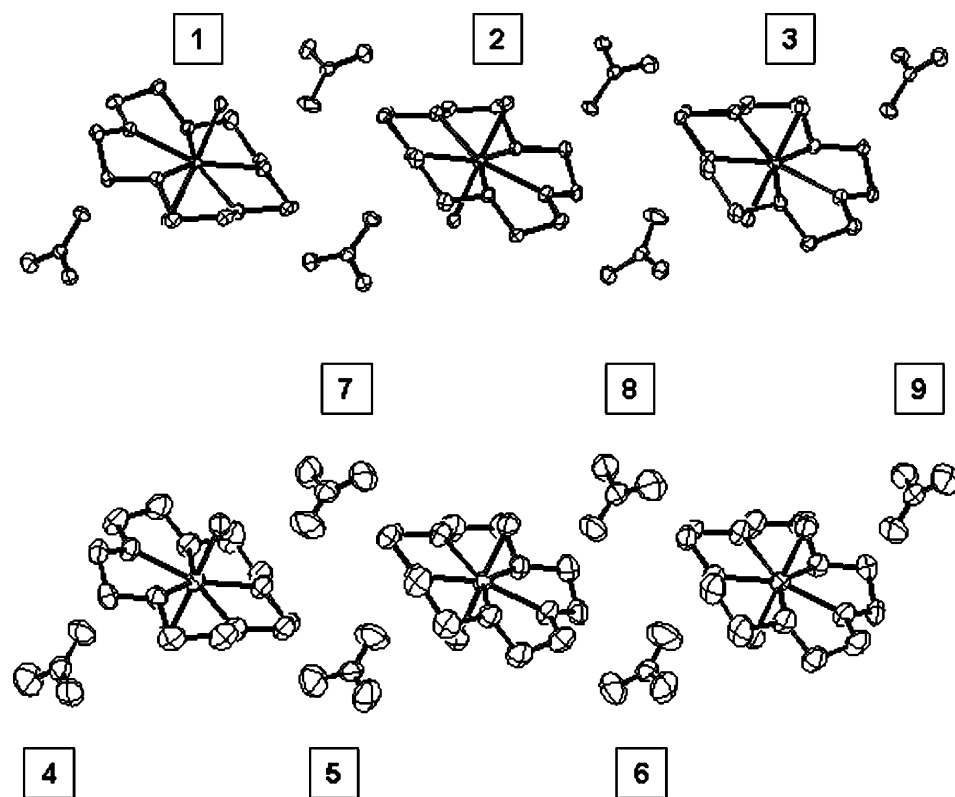
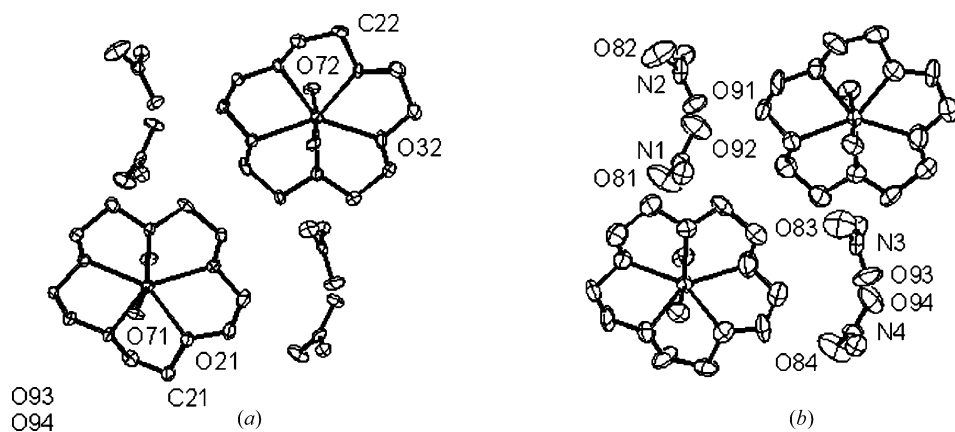


Figure 3

Perspective drawings of the asymmetric unit of the Zn compound, which is viewed along \mathbf{a} at 90 K (upper drawings) and 294 K (lower drawings). The \mathbf{c} axes are horizontal. Ellipsoids are drawn at the 50% level. The atom-numbering schemes for the cation and anion are defined on the upper and lower drawings, respectively. The residue numbers are shown in boxes above or below the ions. The numbers for one C atom in each cation and two O atoms in each of two anions are shown; other atom numbers can be worked out from the translational pseudosymmetry ($\mathbf{c}/3$) and from the overall scheme described in the text.


Figure 4

Perspective drawings of the asymmetric unit of the Mg compound, which is viewed along **a** at 90 K (upper drawings) and 294 K (lower drawings). The **c** axes are horizontal. Ellipsoids are drawn at the 50% level. The atom-numbering schemes for the cation and anion are defined on the upper and lower drawings, respectively. The residue numbers are shown in boxes above or below the ions. The numbers for one C atom in each cation and two O atoms in each of two anions are shown; other atom numbers can be worked out from the translational pseudosymmetry ($\epsilon/3$) and from the overall scheme described in the text.


Figure 5

Perspective drawings of the asymmetric unit of the Co compound, which is viewed along **a** at (a) 90 K and (b) 294 K (righthand drawing). Ellipsoids are drawn at the 50% level. The atom-numbering schemes for the cation and anion are defined on the lefthand and righthand drawings, respectively. Numbers for atoms in the independent cations end in 1 and 2; numbers for atoms in the independent anions end in 1, 2, 3 or 4. The numbers for one C atom and one O atom in each cation and two O atoms in each of two anions are shown; other atom numbers can be worked out from the 2_1 pseudosymmetry (horizontal axis) and from the overall scheme described in the text.

the orientations that are related by the crystallographic pseudosymmetry.

3. Results

3.1. Overview of the packing

In all four structures each water ligand forms hydrogen bonds to two different nitrate ions and each nitrate ion is the hydrogen-bond acceptor for protons from two different cations. In the Cu, Zn and Mg structures the O—H...O bonding networks are two-dimensional and the ions form hydrogen-bonded layers. In the Co structure the O—H...O bonding network is three-dimensional.

This set of structures then includes two (Zn and Mg compounds) that are isostructural (Fig. 6), a third (Cu compound) that is a modulated variant of the first two ($Z' = 5$ rather than 3; Fig. 7), and a fourth structure (Co compound) that is quite different (Figs. 8 and 9).

3.2. Overview of cation geometries

There are $3 + 3 + 5 = 11$ independent cations in the layered structures of the Zn, Mg and Cu compounds; the geometries of these cations are remarkably similar. The 11 cations determined at 90 K were overlaid at 18 match points (all the non-H atoms) using Version 2.1 of the program *CrystMol* (Duchamp, 2004). The r.m.s. deviation for a fit for these 18 points is 0.055 Å; if atoms O6 and O7 are not included (because the M —OH₂ distance depends on the metal) the r.m.s. deviation is a little lower (0.050 Å for 16 match points). The fit of the cations is so good that a plot of the overlaid molecules is uninformative. Even the H atoms of the water ligands fall in nearly the same places.

The conformation of a typical cation in a layered structure is shown in Fig. 10. There is an approximate twofold axis that

Table 2
Average $M-O$ distances (\AA).

M	$\langle M-O_{\text{crown}} \rangle$	$\langle M-OH_2 \rangle$	$\langle M-O6 \rangle$	$\langle M-O7 \rangle$	$\langle M-O7 \rangle - \langle M-O6 \rangle$
Cu	2.253 (14)	1.910 (3)	1.917 (3)	1.902 (1)	-0.014 (3)
Zn	2.227 (13)	1.998 (2)	1.998 (2)	1.987 (1)	-0.011 (3)
Mg	2.193 (11)	2.010 (3)	2.015 (3)	2.004 (1)	-0.011 (3)
Co	2.211 (5)	2.059 (5)	2.070 (1)†	2.049 (1)†	-0.021 (1)

† The labels for atoms O6 and O7 of cation 2 were switched before the averages were taken.

passes through O5, the metal ion and the center of the C3—C4 bond. As there are two lone pairs on each ether O atom, the two C atoms attached on either side should be displaced to the same side of the plane of the five ether O atoms. As the O—C—C—O torsion angles should be about 60° , adjacent C atoms should be alternately above and below the O₅ plane. The odd number of O atoms in the crown ligand, however, means (see diagram in Fig. 10) that it is not possible for all five —CH₂—O—CH₂— groups to adopt the favored arrangement. Strain is evident around the O atom (labeled O5_{*n*}) at the bottom of the ring diagram shown in Fig. 10.

The two cations in the three-dimensionally hydrogen-bonded Co structure are a little different, both from each other and from the cations in the layered structures. The r.m.s. deviation for an 18-point fit of the two cations in the asymmetric unit of the Co compound at 90 K is 0.129 \AA , and the differences between the atom positions, although small, are easy to see (Fig. 11). The r.m.s. deviation for a 16-point fit (water O atoms omitted) for the two cations of the Co structure and the three cations of the zinc structure is 0.138 \AA . The cations in the structures with two- and three-dimensional

hydrogen-bond networks differ in small ways in the region where the crown ligand is strained and in the directions of the hydrogen bonds (see Fig. 12).

3.3. $M-O$ distances

The $M-OH_2$ and $M-O_{\text{crown}}$ distances (see Table 2) are normal (Orpen *et al.*, 1989). The distances vary with the metal, but not in the same way. The $M-O_{\text{crown}}$ distances are shortest for $M = \text{Mg}$, but the $\text{Mg}-OH_2$ distances are second longest. In all cations the $M-O6$ distance is longer than the average $M-O7$ distance, but the average values do not differ much.

The $M-OH_2$ distances vary by 0.10 \AA within the layered monoclinic structures. It is perhaps surprising that the same basic structure type is preserved over such a range of distances.

An analysis of the $M-O_{\text{crown}}$ distances (see Table 3) shows that for the layered structures the metals are closest to the O5 atom (where the ligand strain is greatest) and farthest from atoms O1 and O4. In the Co structure, where the hydrogen-bonding network is three-dimensional, the metal ion seems to be closest to O4 rather than O5, but the differences between $M-O_n$ distances are not as pronounced. The relatively large discrepancy between the two independent Co—O1 distances (as evidenced by the large s.u. in Table 3) may reflect the fact that the orientations of the cations that give the best superposition fit are not the orientations that are related by the crystallographic pseudosymmetry.

3.4. Enantiomeric alternation

The approximate C_2 symmetry of the cations (see Fig. 10) means that individual cations are chiral, although the enan-

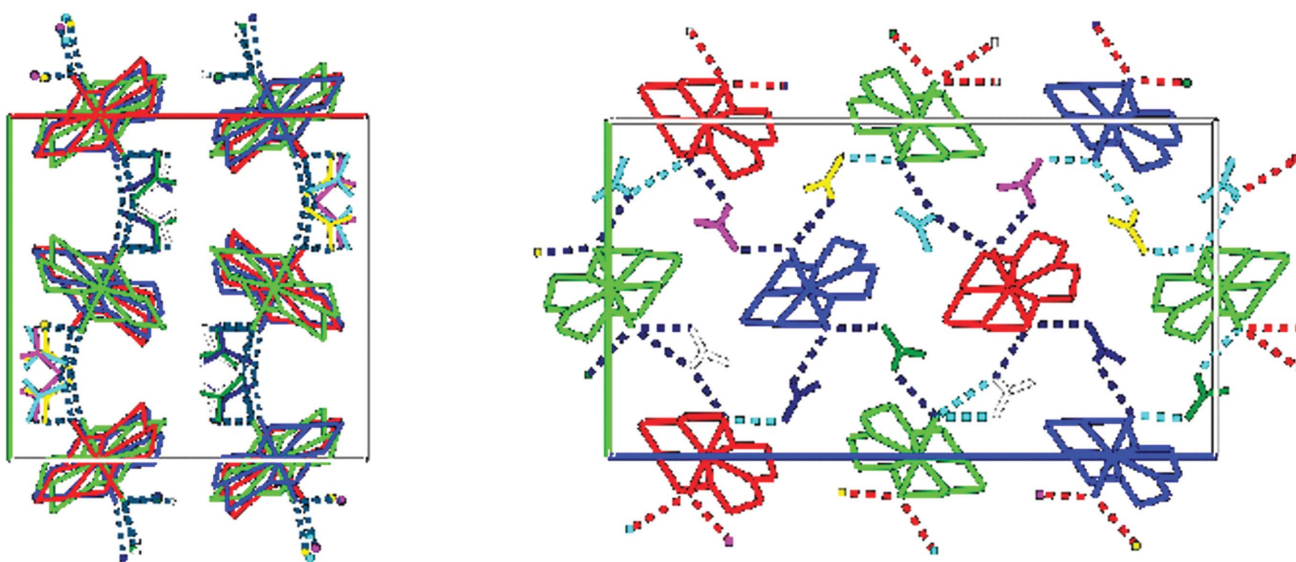


Figure 6

Two projections showing the packing in the Zn and Mg structures drawn with the program *Mercury* (Bruno *et al.*, 2002). The O—H...O hydrogen bonds are shown as dotted lines. The drawing on the left is a projection down c that shows the hydrogen-bonded layers. The drawing on the right is a projection down a of the hydrogen-bonded layer at $x = \frac{1}{4}$ that shows the c glide and the pattern of enantiomeric alternation; in the drawing on the right the c axis is horizontal. Cations 1, 2 and 3 are shown in green, blue and red; the cations in the asymmetric unit have $y \simeq \frac{1}{2}$ and $z \simeq 0, \frac{1}{3}, \text{ and } \frac{2}{3}$.

tiomers would interconvert rapidly in solution and can probably do so in the solid state also if the temperature is not too low. The cations shown in Figs. 6 (Zn and Mg) and 7 (Cu) that ‘point up’ and ‘point down’ within a horizontal row are enantiomers. These conformational enantiomers can be labeled as *R* and *S*.

Consider a row of cations parallel to *c* within one hydrogen-bonded layer of the Zn, Mg and Cu structures. Within these rows cations are in van der Waals contact and are also

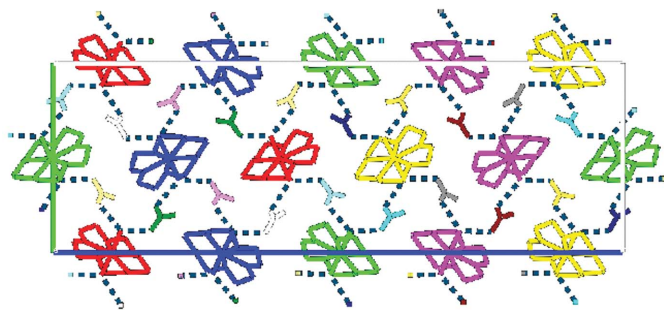


Figure 7

A projection down *a* of a layer at $x = \frac{1}{4}$ of the Cu structure drawn with the program *Mercury* (Bruno *et al.*, 2002); the *c* axis is horizontal. Cations 1–5 are shown in green, blue, red, yellow and magenta; the cations in the asymmetric unit have $y \simeq \frac{1}{2}$ and $z \simeq 0.2n$, $n = 1–5$. Twofold screw axes are found within the layer at $z = \frac{1}{4}$ and $\frac{3}{4}$. The projection down *c* would be very similar to that for the Zn and Mg structures.

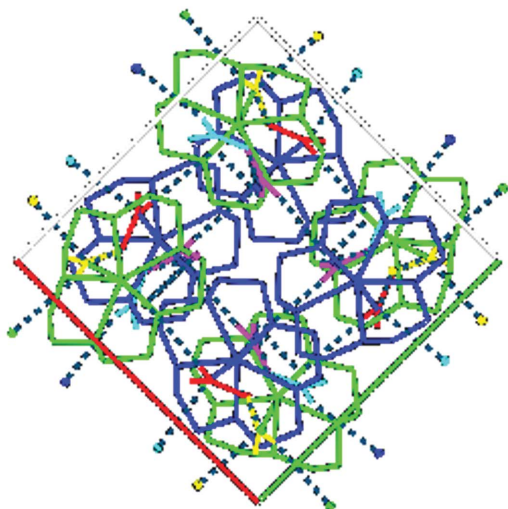


Table 3

Average deviations (Å) from the average $M–O_{\text{crown}}$ distances (see Table 2) for individual O atoms.

<i>M</i>	O1	O2	O3	O4	O5
Cu	+0.075 (2)	−0.029 (5)	−0.004 (4)	+0.071 (3)	−0.113 (1)
Zn	+0.052 (1)	−0.020 (5)	−0.004 (2)	+0.049 (4)	−0.078 (1)
Mg	+0.041 (1)	−0.014 (4)	+0.004 (5)	+0.039 (5)	−0.071 (1)
Co†	+0.010 (18)	+0.008 (8)	+0.005 (3)	−0.017 (2)	−0.005 (4)

† The atom numbers for the Co cations that correspond to the column labels (O1, O2, O3, O4, O5) are O31, O41, O51, O11, O21 and O42, O52, O12, O22, O32. The correspondences were established when the best superposition fit was determined.

connected (albeit indirectly) by $O–H \cdots O$ bonds. The pattern of enantiomeric alternation is *R S S R S S R S S* (or *S R R S R R S R R*) in the $Z' = 3$ structures and *S R S S R S R S S* (or *R S R R S R S R R S*) in the $Z' = 5$ structure. In the $Z' = 3$ structures the enantiomer fails to alternate once in every three pairs of adjacent cations; one in three pairs of cations adjacent in a row is *S S* (or *R R*) rather than *S R* (or *R S*). In the $Z' = 5$ structure the enantiomer fails to alternate once in every five pairs.

3.5. Modulations

The *M* cations of the layered structures all show small (0.0–0.4 Å) displacements from $z = n/Z'$ (e.g. from 0, 1/3 and 2/3 for the Zn and Mg structures). There is a pattern to these

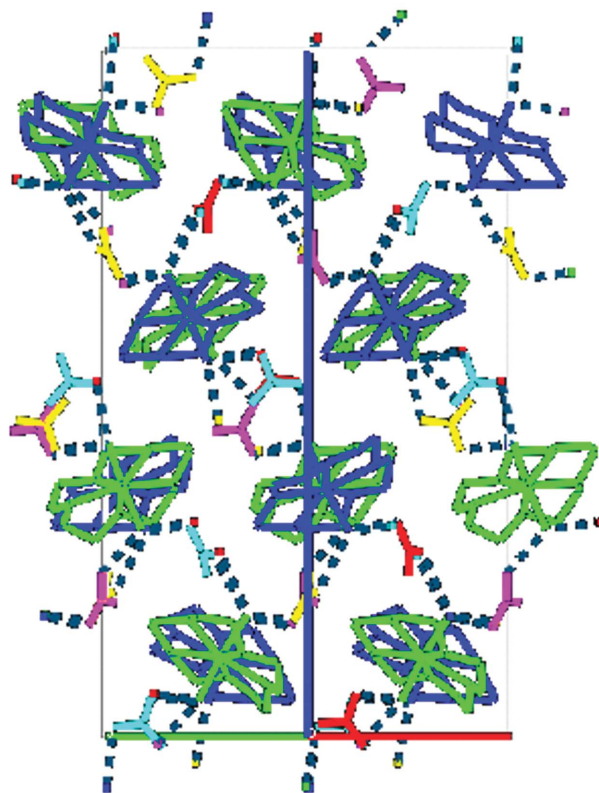


Figure 8

Two projections showing the packing in the Co structure drawn with the program *Mercury* (Bruno *et al.*, 2002). The $O–H \cdots O$ hydrogen bonds are shown as dotted lines. The drawing on the left is a projection down *c*; the drawing on the right is a projection down [110], which is the direction that gives a drawing most like those of the layered structures. Cations 1 and 2 are shown in green and blue.

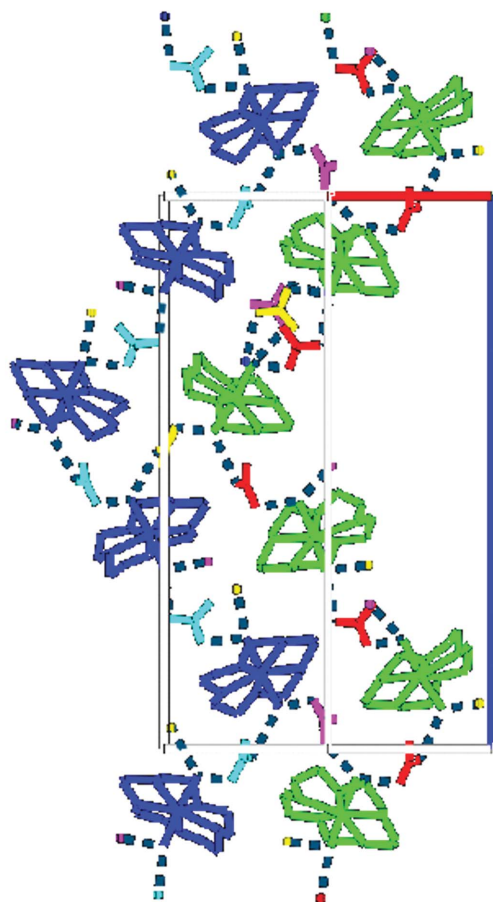
Table 4

Information on the hydrogen bonds between water ligands and the nitrate counterions.

In the case of a bifurcated bond the shorter O...O distance has been used (marked with an asterisk).

<i>M</i>	<i>T</i> (K)	Average O...O (Å)*	Minimum O...O (Å)	Maximum O...O (Å)*	Range (Å)
Cu	88	2.71 (3)	2.66	2.77	0.11
Zn	90	2.76 (8)	2.68	2.97	0.28
Mg	90	2.78 (8)	2.71	2.98	0.27
Co	90	2.77 (3)	2.73	2.83	0.10
Cu	294	2.76 (5)	2.68	2.87	0.19
Zn	294	2.80 (8)	2.73	2.97	0.24
Mg	294	2.84 (8)	2.76	3.01	0.25
Co	294	2.80 (5)	2.72	2.88	0.16

displacements that is most apparent if two cations in adjacent rows and connected through a single nitrate ion are considered. If those two cations 'point towards' each other (see Figs. 6 and 7) then the distance along *c* between the two metal ions

**Figure 9**

Projection down $[1\bar{1}0]$ of part of the packing in the Co structure. The 4_1 helices of cation 1 (green) are linked by the nitrate anion 1 (red), while the helices of cation 2 (blue) are linked by anion 4 (lighter blue). The centers of the helices are offset by $\Delta x = \Delta y = \pm \frac{1}{2}$; the two helices are linked to each other and to other helices by anions 2 (yellow) and 3 (magenta).

is shorter than average. If the two cations 'point away' from each other that distance is larger than average. The displacements appear to be a response to the most important modulation, which is the pattern of enantiomeric alternation.

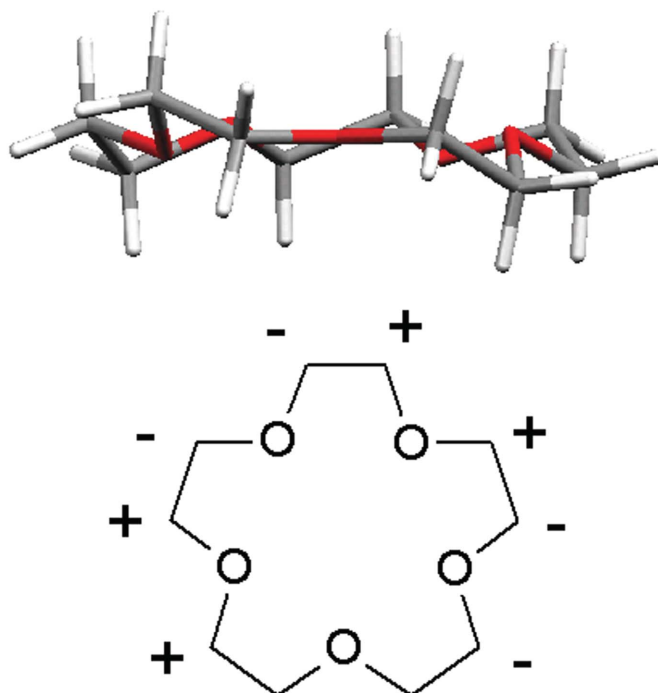
There are also considerably smaller, but systematic, displacements of the metal ions from $x = \frac{1}{4}$ (0.0–0.1 Å) and $y = \frac{1}{2}$ (< 0.1 Å).

These modulations have been and will be discussed (Hao *et al.*, 2005*a,b*) as part of a general discussion of the possible and the observed patterns of enantiomeric alternation.

3.6. O—H...O hydrogen bonds

All water ligands form O—H...O bonds to nitrate ions (see Table 4). Nitrate ions normally form two O...H—O bonds to water ligands through two different O atoms (see chemical line drawing and Fig. 7). In the $Z' = 3$ structures, however, there is a bifurcated bond (O8_7 and O10_7 to O6_1; distances 3.00 and 2.97 Å at 90 K, and 2.97 and 3.00 Å at 294 K) and a bond in which a single nitrate O atom (O9_6) interacts with two water ligands (O6_3 and O7_1; distances 2.83 and 2.79 Å at 90 K, and 2.97 and 2.83 Å at 294 K) (see also Fig. 6).

The unusual O—H...O bonds occur between cations that 'point towards' each other. The distance between metal ions in such pairs of cations is smaller than average (see §3.5), so that there seems to be insufficient space for the anions to use two different O atoms to make O...H—O bonds. These unusual

**Figure 10**

A drawing of the crown ligand as it is found in the three structures with two-dimensional hydrogen-bond networks and a diagram showing the displacements of the C atoms from the plane of the five O atoms. The O atom in the region that is most strained, O5_{*n*}, is in the front of the drawing of the ligand and at the bottom of the diagram.

hydrogen bonds, however, are longer than average (see Table 4).

If the reason for the formation of unusual O—H...O bonds in the Zn and Mg structures is understood, then why are no unusual bonds found in the Cu structure? The answer to this question requires a more detailed analysis of the structural modulations than can be presented in this paper.

The variation with temperature of the O...O distances is significant. When the temperature of the Cu, Zn and Mg crystals is increased above 310 K new phases that are structural variants of the phases described here are found (Hao *et al.*, 2005b).

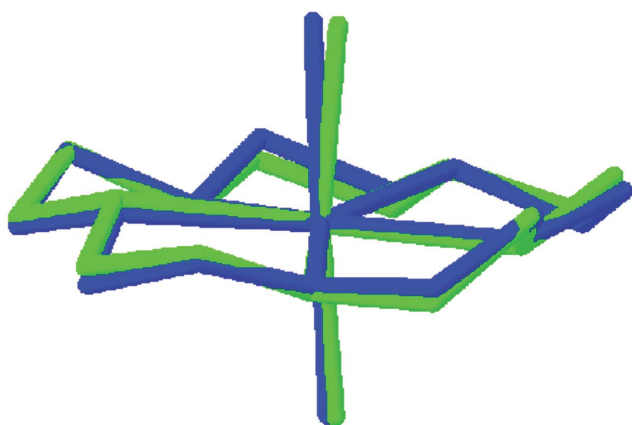


Figure 11
Overlay (see text) of the two cations of the Co structure as determined at 90 K. Cation 1 is shown in green and cation 2 in blue. The O atoms in the region of the crown ligand that is most strained, O21 and O32, are in the front of the drawing.

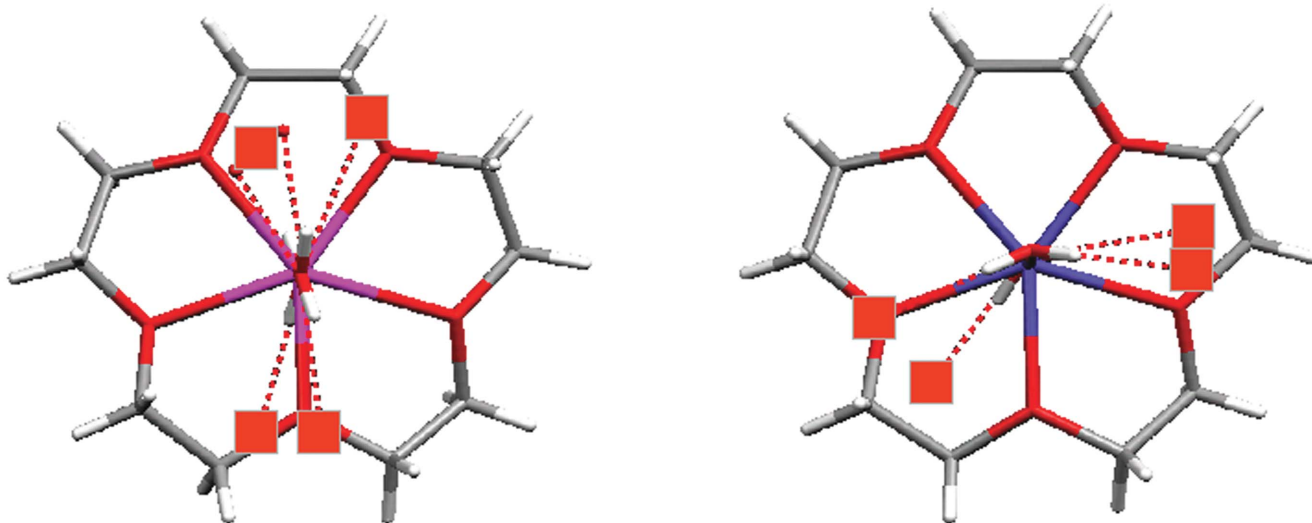


Figure 12
Drawings of typical cations in (left) the structures (Zn, Mg and Cu) in which the hydrogen-bonding pattern is two-dimensional, and (right) in the structure (Co) in which the pattern is three-dimensional. There are subtle difference between the two types of cation in the region (at the bottom of the drawing) in which the crown ligand is most strained. The locations of the O—H...O bonds to adjacent nitrate ions are also shown.

4. Discussion

The four $[M(H_2O)_2(15\text{-crown-5})](NO_3)_2$ structures discussed here are unusual in that they all have similar hydrogen-bond patterns, that they fall into two structure types and that the layered structure type has two variants. All four have unusual Z' values (2, 3 and 5). It is also surprising that the original determinations of the four structures were all incorrect in some important way.

4.1. What went wrong previously?

4.1.1. $M = Cu$. The first report of the structure of this compound (Dejehet *et al.*, 1987b) gave the unit cell we observe, but failed to find the inversion centers. In 1987 there were no widely available algorithms for checking symmetry (such as, *e.g.* is now found in *PLATON*; Spek, 2003), so that finding the missing symmetry centers, which could be located at any of ten sets of positions, would have been an arduous task.

The second structure report (Rogers & Song, 1995) gave a unit cell five times smaller and a very disordered structure. Those authors knew about the possibility of a larger unit cell, but did not mention having seen extra diffraction peaks (data for Mo $K\alpha$ radiation collected at room temperature using a Nonius CAD-4 diffractometer). The use by Dejehet *et al.* (1987b) of Cu $K\alpha$, rather than Mo $K\alpha$, radiation was probably the determining difference; doubling the wavelength leads to an order of magnitude increase in intensity and significantly greater attainable resolution in θ for these crystals. If Rogers & Song (1995) looked at a very small crystal and took no axial photographs then the superstructure reflections might easily have been missed.

It is also possible that the automated search routine of the CAD-4 software found intensity corresponding to the larger

cell, but that the peak centering and autoindexing routines failed to handle that intensity well. If h is even, the $\lambda = 5n \pm 1$ reflections are 250 times weaker than the $\ell = 5n$ reflections and the $\ell = 5n \pm 2$ reflections are weaker still. On the other hand, for the h odd reflections, the $\ell = 5n$ reflections are the weakest, the $\ell = 5n \pm 1$ reflections are two–three times stronger on average and the $\ell = 5n \pm 2$ reflections are more than 20 times stronger. The result is a diffraction pattern that can easily be interpreted as being B -centered (see Fig. 13), but for which the exact locations of the apparent h odd reflections, which are actually composites, depend on the relative intensities of adjacent reflections having $\ell = 5n + 2$ and $\ell = 5n + 3$. As \mathbf{c} is so long ($c > 43 \text{ \AA}$), reflections with the same h and k and with ℓ values that differ by 1 may have been poorly resolved in the original study, especially if the diffractometer was run in default mode. The resolution problem is most acute for the h odd, $\ell = 5n + 2$ and $\ell = 5n + 3$ reflections. We suspect that the

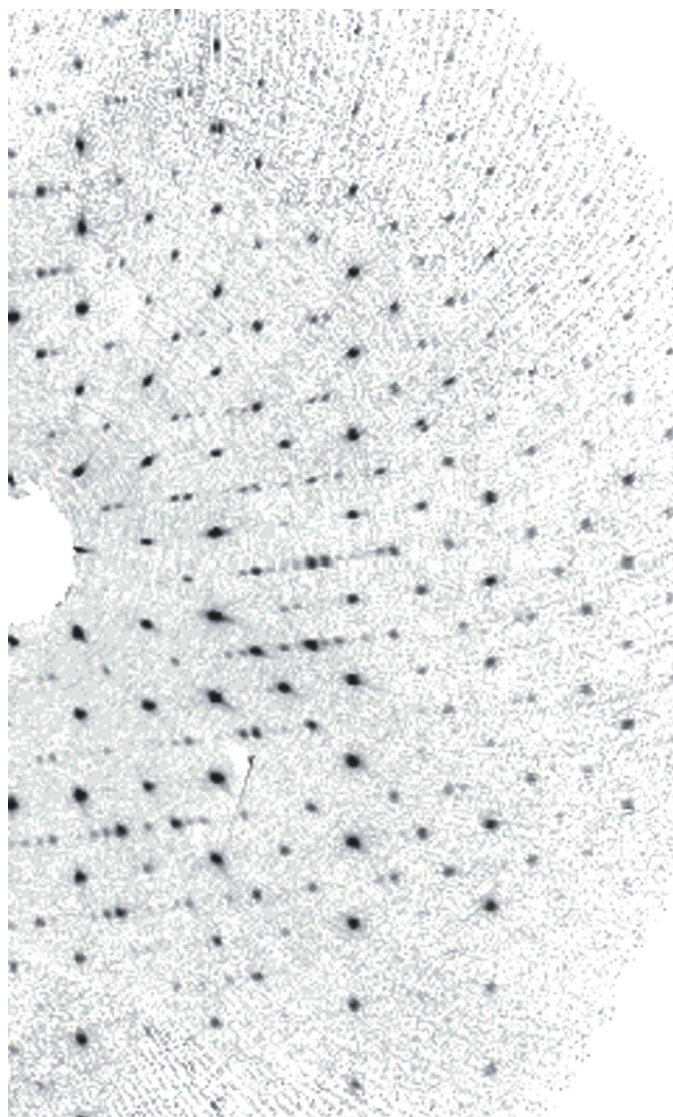


Figure 13

Part of a reconstructed $h1\ell$ plane of the reciprocal lattice of the Cu structure measured at 294 K. The \mathbf{a}^* axis points vertically upwards; the \mathbf{c}^* axis points to the right and slightly upwards.

CAD-4 indexing software simply removed the h -odd peaks from the list of reflections on which the cell was based.

The non-integral ratio (4.89) between the lengths c for the cell choices Pc ($Z' = 10$) and $P2_1/c$ ($Z' = \frac{1}{2}$) and the different β angles (102.2° versus 97.35°) for those choices could also have caused confusion. The strong similarity in cell constants between the larger and smaller Cu unit cells is more obvious if a transformation is made, e.g. the larger Pc (actually, $P2_1/c$) cell is transformed to a Pn (actually, $P2_1/n$) cell.

A superspace description of the Cu-containing structure was published recently by Schönleber & Chapuis (2004), who also redetermined the structure. These authors considered the possibility of inversion symmetry, but dismissed it, presumably because they did not recognize the required origin shift.

4.1.2. $M = Zn$. The original authors (Dejehet *et al.*, 1987a) failed to find the inversion centers that change the space group from Pc ($Z' = 6$) to $P2_1/c$ ($Z' = 3$). In this structure there are six, rather than ten, possible sets of positions for the inversion centers, but in the absence of an automated search procedure, finding the missing symmetry would not have been easy.

4.1.3. $M = Mg$. The published structure has the origin displaced by about $\frac{1}{4}$ along \mathbf{a} , so that one of the three cations is located on an inversion center. The consequent disorder is not mentioned in the paper (Junk & Steed, 1999). Various warning signs ($R = 0.11$; $wR = 0.25$; very eccentric ellipsoids; s.u.s for bond lengths that are very large for a structure determined at 100 K) seem to have been ignored. The structure of the isostructural Zn compound, which was in the CSD, was not mentioned. A recent re-examination (Steed, 2004) of the original data indicates that the correct structure solution was overlooked.

4.1.4. $M = Co$. This structure was first reported (Holt *et al.*, 1981) as being in the space group $P4_12_12$ with $a = 8.079$ and $c = 27.231 \text{ \AA}$ at 291 K. The 15-crown-5 ligand was described as disordered over two sites. Data were measured for Mo radiation using a Syntex $P2_1$ diffractometer.

The reflections found by Holt *et al.* (1981) correspond to the $h + k = 2n$ reflections of the larger cell [$\mathbf{a}_{\text{new}} = (110/\bar{1}10/001) \mathbf{a}_{\text{old}}$]. We find that at 294 K the $h + k = 2n + 1$ reflections are *ca* 8 times weaker than the $h + k = 2n$ reflections at $\sin \theta/\lambda = 0.10 \text{ \AA}^{-2}$ ($\theta = 13^\circ$ for Mo $K\alpha$ radiation) and are about 7 times weaker at $\sin \theta/\lambda = 0.36 \text{ \AA}^{-2}$ ($\theta = 25^\circ$ for Mo $K\alpha$ radiation). If the crystal used by Holt *et al.* was small then the extra reflections could easily have been missed. Even if the reflections had been noticed it might have been very difficult to do a satisfactory refinement because the least-squares programs available did not usually have options for including restraints or twinning.

We have very recently discovered (Hao *et al.*, 2005b) that the Co-containing compound undergoes a phase transition at *ca* 306 K to the disordered $P4_12_12$ structure reported at 291 (2) K by Holt *et al.* (1981).

4.1.5. Prediction. We suspect that the frequency of structures with $Z' > 1$ will appear to increase now that diffractometers equipped with area detectors have become standard. In the two decades during which most crystal structures were determined from data measured with serial diffractometers

equipped with scintillation detectors and running auto-indexing software in default mode, the scattering between strong Bragg peaks was largely ignored. Even if weak 'extra peaks' were found and indexed, it was often difficult or impossible to measure their intensities well enough for a satisfactory refinement in a larger unit cell. The efficiency of CCD and image-plate detector data collection schemes seem to result in better counting statistics overall than were typical of scintillation counters and the average intensity of the incoming radiation has risen. Furthermore, the software used to process the raw images has much more information to work with than did the auto-indexing routines of 30 years ago. Classes of reflections that are systematically weak, or even very weak, are much less likely to be missed.

4.2. Other 15-crown-5 structures

A simple survey of the CSD showed that the 15-crown-5 ligand is quite often registered as disordered. We suspect that at least some of these reported structures are incomplete descriptions of the true structures.

The other compounds of the type $[M(\text{H}_2\text{O})_2(15\text{-crown-5})]A_m$, where A is a hydrogen-bonding anion, typically have extended hydrogen-bond patterns that are one- rather than two-dimensional. The two- and three-dimensional hydrogen-bonded structures in this series of compounds are unique. The size of the nitrate counterion must be important in stabilizing these structures.

4.3. Why are the structures modulated?

A very careful consideration of the interionic contacts in the layered structures shows that the positions of the methylene H atoms of the 15-crown-5 ligand complicate the crystal packing. Adjacent cations that are in different hydrogen-bonded layers (*i.e.* cations that are adjacent along **a**) should be related by at least approximate inversion symmetry. The centroids of cations that are adjacent in a row (*i.e.* cations that are adjacent along **c**) can be closest if their 'points' (C3_n and C4_n in one cation and C3_m and C4_m in the other) are adjacent across a local inversion center, but must be farther apart if their 'tails' (C8_n and C9_n) are adjacent. If a 'point' is adjacent to a 'tail' the spacing is intermediate.

The spacing of the metal ions in a row should be even so that the lengths and angles of all the $\text{O}-\text{H}\cdots\text{O}$ bonds can be optimized. There is a conflict, however, between the requirement for even spacing of the metal ions and for good packing of the 15-crown-5 ligands. This subject will be explored in more detail in future papers (Hao *et al.*, 2005a,b).

5. Conclusions

The existence of the $P2_1/c$, $Z' = \frac{1}{2}$ phase reported for $[\text{Cu}(\text{H}_2\text{O})_2(15\text{-crown-5})](\text{NO}_3)_2$ (Rogers & Song, 1995) is doubtful.

Structures in which there is major disorder should be viewed with suspicion, especially if there is a low-energy pathway between the disordered components, if the temperature is low and if the data were measured with a serial diffractometer using Mo $K\alpha$ radiation.

The $[M(\text{H}_2\text{O})_2(15\text{-crown-5})](\text{NO}_3)_2$ system is likely to be rich in polymorphs and modulated variants.

We thank Professors R. D. Rogers and J. W. Steed for helpful discussions.

References

- Allen, F. H. (2002). *Acta Cryst.* **B58**, 380–388.
- Brock, C. P. & Patrick, B. O. (2002). *Mol. Cryst. Liq. Cryst.* **389**, 79–85.
- Bruno, I. J., Cole, J. C., Edgington, P. R., Kessler, M., Macrae, C. F., McCabe, P., Pearson, J. & Taylor, R. (2002). *Acta Cryst.* **B58**, 389–397.
- Dejehet, F., Debuyst, R., Wei, Y. Y., Declercq, J. P. & Tinant, B. (1987a). *J. Chim. Phys. Phys.-Chim. Biol.* **84**, 107–113.
- Dejehet, F., Debuyst, R., Wei, Y. Y., Declercq, J. P. & Tinant, B. (1987b). *J. Chim. Phys. Phys.-Chim. Biol.* **84**, 975–979.
- Duchamp, D. J. (2004). *CrystMol*, Version 2.1. D and A Consulting LLC, Kalamazoo, Michigan, USA.
- Flack, H. D. (1983). *Acta Cryst.* **A39**, 876–881.
- Hao, X., Siegler, M. A., Parkin, S. & Brock, C. P. (2005a). *Cryst. Growth Des.* In the press.
- Hao, X., Siegler, M. A., Parkin, S. & Brock, C. P. (2005b). Unpublished results.
- Herbstein, F. H. (2000). *Acta Cryst.* **B56**, 547–557.
- Holt, E. M., Alcock, N. W., Hendrixson, R. R., Malpass Jr, G. D., Ghiradelli, R. G. & Palmer, R. A. (1981). *Acta Cryst.* **B37**, 1080–1085.
- Junk, P. C. & Steed, J. W. (1999). *J. Chem. Soc. Dalton Trans.* pp. 407–414.
- Li, Y. (1996). *Bull. Chem. Soc. Jpn.* **69**, 2513–2523.
- Nonius (1999). *Collect.* Nonius BV, Delft, The Netherlands.
- Orpen, A. G., Brammer, L., Allen, F. H., Kennard, O., Watson, D. G. & Taylor, R. (1989). *J. Chem. Soc. Dalton Trans.* pp. S1–S83.
- Otwinowski, Z. & Minor, W. (1997). *Methods Enzymol.* **276**, 307–326.
- Rogers, R. D. & Song, Y. (1995). *J. Coord. Chem.* **34**, 149–157.
- Schönleber, A. & Chapuis, G. (2004). *Ferroelectrics*, **305**, 99–102.
- Sheldrick, G. M. (1994). *SHELXTL PC*. Siemens Analytical Instruments, Inc., Madison, Wisconsin, USA.
- Sheldrick, G. M. (1997a). *SHELXS97*. University of Göttingen, Germany.
- Sheldrick, G. M. (1997b). *SHELXL97*. University of Göttingen, Germany.
- Spek, A. L. (2003). *J. Appl. Cryst.* **36**, 7–13.
- Steed, J. W. (2004). Personal communication.
- Xia, A., Selegue, J. P., Carrillo, A., Patrick, B. O., Parkin, S. & Brock, C. P. (2001). *Acta Cryst.* **B57**, 507–516.
- Xia, A., Selegue, J. P., Carrillo, A., Patrick, B. O., Parkin, S. & Brock, C. P. (2002). *Acta Cryst.* **B58**, 565.